Available online www.jsaer.com

***Journal of Scientific and Engineering Research*, 2019, 6(4):144-152**

Research Article

ISSN: 2394-2630
CODEN(USA): JSERBR

Spectroscopic Study of $xSiO_2$ $(1-x)Sb_2O_3$ for x= 10%, 20%, 30%, 40% and 50% mol% as Quench Glass and Glass Ceramics

M. Abdur Rashid[1], M. Murshidul Islam[1], M. Abu Asif Saiham[1], M. Rafiqul Ahsan[1], M. G. Mortuza[1], Mirza H. K. Rubel[2]

[1]Department of Physics, University of Rajshahi, Rajshahi–6205, Bangladesh
[2]Department of materials science and Engineering University of Rajshahi, Rajshahi–6205, Bangladesh

Abstract The infrared absorption spectra of $xSiO_2$ $(1-x)Sb_2O_3$ for x= 10%, 20%, 30%, 40% and 50% mol% glass systems are examined in the region 400 to 4000 cm^{-1} together with X ray diffraction and interpreted structurally in terms of chemical bonding. Absorption bands and mode attributions have been fully discussed. Absorption frequencies and intensities are found to be strongly and systemically dependent on glass composition. The abrupt changes in the infrared spectra are observed with the increase of SiO_2. The spectra of SiO_2 (40, 50 mol%) containing glasses show an increased number of distinct peaks in the low frequency region (400-1400cm^{-1}) with a convolution of broad Gaussians in the high frequency region (1400-4000cm-1). All the spectra are baseline corrected and overlapped Gaussians are deconvoluted to appropriate number of Gaussians using computer program. From FT-IR spectra different significant absorption, stretching and vibrational bands are observed as peaks in the low and high frequency regions of the spectra. The distinct peaks and the peak position of the deconvoluted Gaussians are assigned to O-Si-O, Si-O-Si, O-H, Si-O bands and SbO_3 (trigonal pyramids), β-Sb_2O_4 groups. The compositional dependence of the band positions with SiO_2 concentration for $xSiO_2$ $(1-x)Sb_2O_3$ glass system is also plotted which reveals a positive correlation with SiO_2 content. It is investigated by the FTIR spectroscopy that the peaks of the heat treated glasses shifted more with increasing of SiO_2 comparatively the peaks of the base glasses. The X-ray diffraction patterns of the base and heat treated samples (20S80Sb, 50S50Sb) indicate that the samples are partially crystalline.

Keywords Si/Sb-based glass, X-ray diffraction, FT-IR analysis, Deconvoluted spectra

1. Introduction

It is well known that FTIR absorbance or IR spectra of alkali silicate glasses which are solidified super cooled solutions of various metallic silicates having infinity viscosity, partially amorphous, transparent and translucent substance provide significant, valuable useful qualitative and quantitative information on the arrangement of atoms, the nature of chemical bonding between them, the change in atomic configurations caused by increases or decrease of concentration of materials forming system. Alkali metal or divalent metal oxide with silica forms an attractive family of insulating glassy materials. These are called potential candidates for many desirable applications in optical systems because of their interesting optical properties [1]. In the present work in structure of antimony silicate glasses, silicon oxygen tetrahedrons [SiO_4] and pseudo tetrahedrons [SiO_3] joined to each other. In these glass system, Antimony acts as a network formers and play a dramatic role as they possess some exciting properties like high refractive index, large transmission window, large non-linear optical properties, low phonon energy and high dielectric constant [2]. In $xSiO_2$ $(1-x)$ Sb_2O_3 $(0.1\leq x\leq 0.5)$ glass system, molten Sb_2O_3 when cooled rapidly produces a clear transparent glass [3]. A substantial amount of Sb_2O_3 can be dissolved in other glass forming oxides like SiO_2, B_2O_3, P_2O_5 etc; usually these binary mixtures are low melting,

and various antimony (III) compounds having high vapor pressures are available with high purity. Unfortunately the structural role of Sb_2O_3 in glass forming melts is not clearly known. Thus in this investigation we have studied the FTIR spectra and XRD spectra of $xSiO_2$ $(1-x)Sb_2O_3(0.1\leq x\leq 0.5)$ glass system.

2. Experimental Procedure

There are various experimental methods usually employed to explore the glass structure. For the preparation of $xSiO_2$ $(1-x)$ Sb_2O_3 or $xS(1-x)Sb$ glass system, the commercially available raw material SiO_2 and heavy material Sb_2O_3 were selected as initial materials expressed in mol%. The powder raw material of appropriate amounts, usually 10gm batches, were first finished dust by mortar and pestle then homogenized by rolling and shaking on a ball milled machine for 6-8 hours and then disk of approximately 1gm solution for each sample prepared by hydraulic press was melted by oxyacetylene flame [4]. In this work mainly IR and XRD are used to characterize the materials. Infrared spectroscopes give absorption spectra characteristic of motions of atom-atom bonds. The resulting absorption bands are like fingerprints of particular structural arrangement. The qualitative and quantitative analysis of the IR absorption spectra is employed with the deconvolution to several Gaussians to characterize the materials. In X-Ray diffraction technique the measured pair distribution functions can be compared to the distribution functions calculated from models of the glass structures. Glass ceramics can be produced from the base glasses by carefully controlled heat treatment. To prepare it some quantity of the x $SiO_2(1-x)Sb_2O_3$ base glasses were first pulverized in a mortar and then heat treated the fine powder base glass at 700 ^{0}C for 12 hours in an electric furnace. To collect IR spectra of a sample various techniques can be employed for placing the sample in the path of infrared beam depending upon whether the sample is gas or solid or liquid. For glassy material $xSiO_2$ $(1-x)Sb_2O_3$, KBr pellet technique is well-established [5,6,7]. In this work glass samples were grounded in a clean mortar to a fine powder and weighed quantity (~0.003gm) of the powder was mixed intimately with desiccated highly purified (~99.99%) alkali halide, KBr powder (~0.02gm). The mixture was then pressed with a pressure of 2 tons per square inch to yield a transparent pellet of approximate thickness 0.01mm suitable for mounting in the spectrometer. All infrared spectra of the glasses were collected on a Shimadzu Model IR Prestige – 21 PC spectrophotometer over the range of wave number 4000cm^{-1}-400cm^{-1}.

Table 2.1: Nominal composition, melting temperature and optical quality of glasses of various compositions

Title of the samples	Nominal composition in mole%		Melting temp. in ^{0}C	Optical quality	XRD
	SiO_2	Sb_2O_3			
10S90Sb	10	90	Unknown	Opalescent, Yellow	NI
20S80Sb	20	80	Unknown	Opalescent, Yellow	Partially Crystalline
30S70Sb	30	70	Unknown	Opalescent, Yellow	NI
40S60Sb	40	60	Unknown	Opalescent, Yellow	NI
50S50Sb	50	50	Unknown	Opalescent, Yellow	Partially Crystalline

S = SiO_2, Sb = Sb_2O_3, NI = Not Investigated.

3. Results

The FTIR absorbance spectra of different $xSiO_2(1-x)Sb_2O_3$ glass system are recorded between 400 to 4000 cm^{-1} of the base glass samples and heat treated samples which are shown in figure 3.1 (a) and (b) respectively. The spectra of the present samples are divided into two regions; one is the lower wave number in the frequency range 400-1400cm^{-1} which are the different vibration modes of structural group's related absorption and the other in the higher wave number in the frequency range 1400-4000cm^{-1} which are the water related absorption. This figure should facilitate any quick comparison to enable one to draw important conclusions about the changes in the structural units of the base samples and also compare base and heat treated samples. For finding the exact position of the absorption band, the deconvolution process of these bands is considered which are shown in figure 3.2(a) ,(b),(c),(d),(e),(f),(g),(h),(i) and (j).The positions of the prominent absorption peaks of each base and heat treated samples are summarized in table-1. Relative areas of the chemical bonds of the $xSiO_2(1-x)Sb_2O_3$ base glasses and heat treated glass are also shown table-2 and graph respectively 3.3 (a) and (b). Variation of band position with SiO_2 concentration of base samples are also shown in Figure 3.4(a) and (b).

X-ray powder diffraction (XRD) which is a rapid analytical technique is used for phase identification of a crystalline material and can provide information on unit cell dimensions and also shown in figure 3.5 (a) and (b).

Table 3.1: Comparison of the main IR absorption bands observed in base and heat treated glasses with related glasses and crystalline phases

Remarks	**Structural group**	**Absorption band (cm^{-1})**	**Corresponding references**
Stretching vibration	O-Si-O	445	[14]
		435-442	[present work]
Bending Vibration	Si-O-Si	490,440,465,470	[11],[15],[16],[17]
		461-468	[present work]
Asymmetric Bending Vibration	SbO_3 Valentinite	470,455,492,455-485	[8],[11],[10],[9]
		499-503	[present work]
Symmetric Bending Vibration	SbO_3 Valentinite	540,600,546,540	[8],[12],[10],[9]
		544-552	[present work]
Asymmetric Stretching Vibration	SbO_3 Valentinite	600,590,592	[18],[8],[10]
		590-628	[present work]
Symmetric Stretching Vibration	SbO_3 Valentinite	690,700,692,	[8],[12],[10]
		691-693	[present work]
Symmetric Stretching Vibration	SbO_3	740,925,675-740	[8],[12],[9]
	Senarmontite	739-787	[present work]
Stretching Vibration	SbO_3	940,925	[19],[20]
	Senarmontite	892-951	[present work]
Asymmetric Stretching Vibration	Si-O	1040,1037	[9],[13]
		1030-1063	[present work]
Stretching Vibration	Si-O-Si	1180,1160,1132-1236	[15],[21],[17]
		1173-1189	[present work]
Cerventinite	β-Sb_2O_4	650	[9]
		642-687	[present work]
Bending Vibration	O-H	1640,1620-1640,1610-1650,1600-1660	[22],[23],[24],[25]
		1637-1648	[present work]
Stretching Vibration	H-O-H	3420-3437,3400,2857-3571,3400-3600	[6],[22],[26],[24]
		3435-3456	[present work]

Table 3.2: Relative areas of the chemical bonds of the $xSiO_2(1-x)Sb_2O_3$ base and heat treated glasses.

Assignment	Relative areas (base samples)					Relative areas (heat treated samples)				
	10S90Sb	20S80Sb	30S70Sb	40S60Sb	50S50Sb	10S90Sb	20S80Sb	30S70Sb	40S60Sb	50S50Sb
Si-O-Si (b-v)	5.6	21.75	20.90	17.42	10.43	4.18	18.91	5.97	11.8	10.51
SbO_3(as-b)valentinite		4.65	6.02		1.16					
SbO_3(s-b)valentinite		22.40	19.48	10.06	3.50					
SbO_3(as-s)valentinite	24.75	4.46	8.41	5.38	4.57	15.26	7.20	2.50	5.18	1.52
SbO_3(s-s)valentinite		8.99	10.42	6.33	4.77	5.12	3.84	5.92	26.52	4.84
SbO_3(s-s)senarmontite	5.96	7.24	6.37	8.27	8.11	5.12	3.84	5.92	26.52	4.84
SbO_3(s-v)senarmontite	10.26	10.79	10.03	17.87	16.57	11.77	0.60	13.21		7.02
Si-O (as-s)	33.16	13.77	12.70	32.09	47.07	34.94	5.48	42.19	33.95	6.96
Si-O-Si (s-v)	20.27					23.20	0.92	6.73		5.15

Where, s-s= symmetric stretching vibration as-s= asymmetric stretching vibration
s-b= symmetric bending vibration as-b= asymmetric bending vibration
b-v= bending vibration s-v= stretching vibration

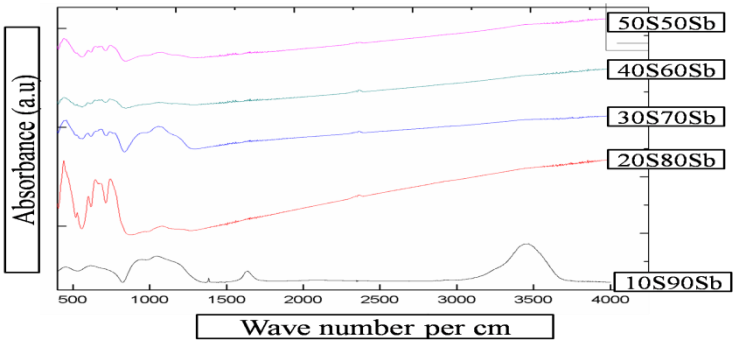

Figure 3.1(a): Infrared spectra of $xSiO_2(1-x)Sb_2O_3$ of base samples

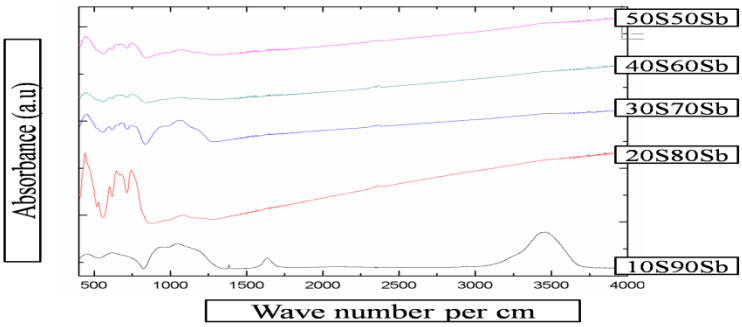

Figure 3.1(b): Infrared spectra of $xSiO_2(1-x)Sb_2O_3$ of heat treated samples

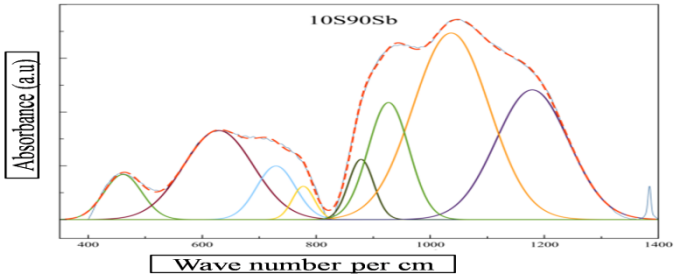

Figure 3.2(a): Deconvoluted spectra of 10S90Sb base sample

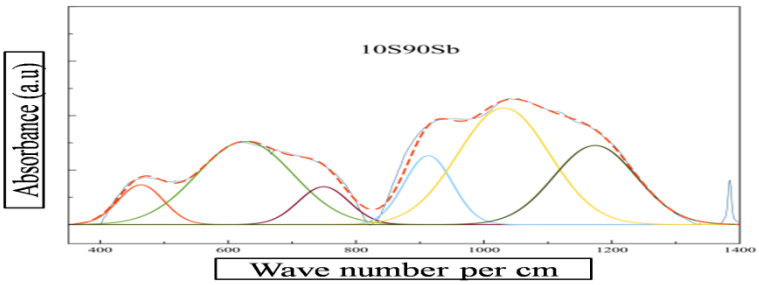

Figure 3.2(b): Deconvoluted spectra of 10S90Sb heat treated sample

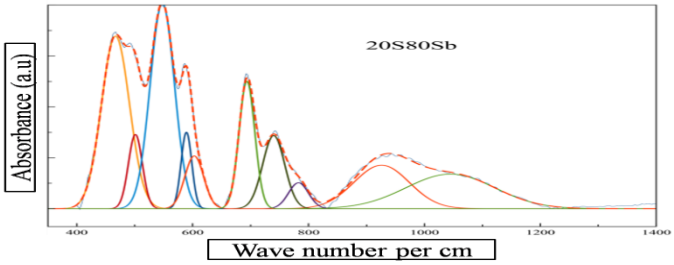

Figure 3.2(c): Deconvoluted spectra of 20S80Sb base sample

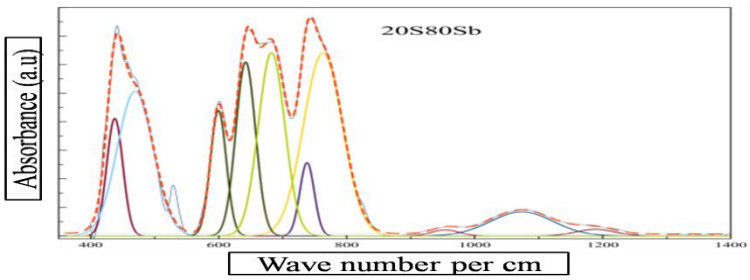

Figure 3.2(d): Deconvoluted spectra of 20S80Sb heat treated sample

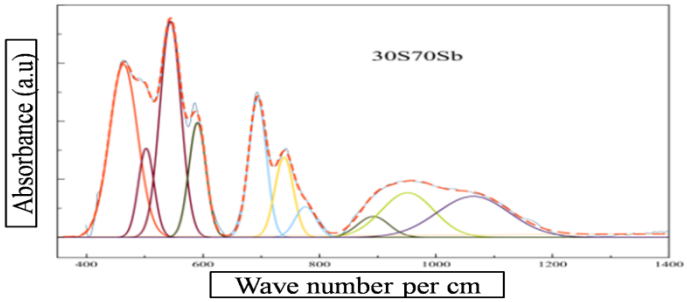

Figure 3.2(e): Deconvoluted spectra of 30S70Sb base sample

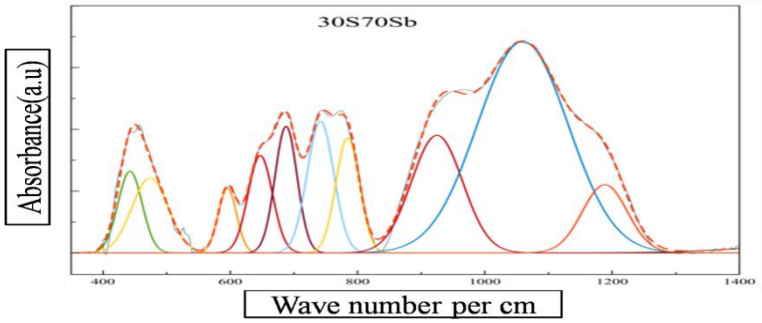

Figure 3.2(f): Deconvoluted spectra of 30S70Sb heat treated sample

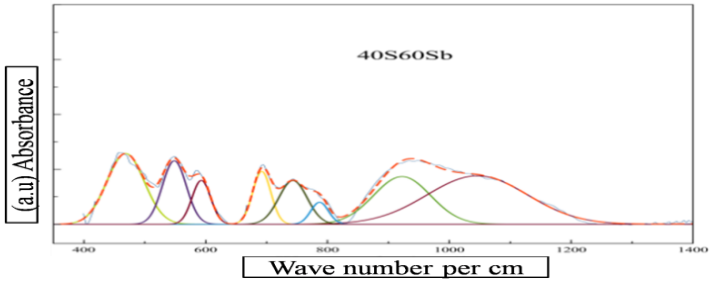

Figure 3.2(g): Deconvoluted spectra of 40S60Sb base sample

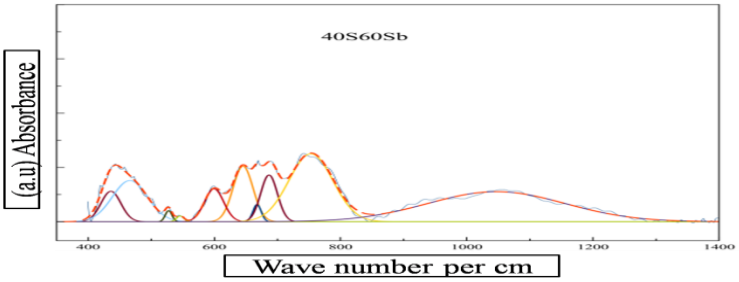

Figure 3.2(h): Deconvoluted spectra of 40S60Sb heat treated sample

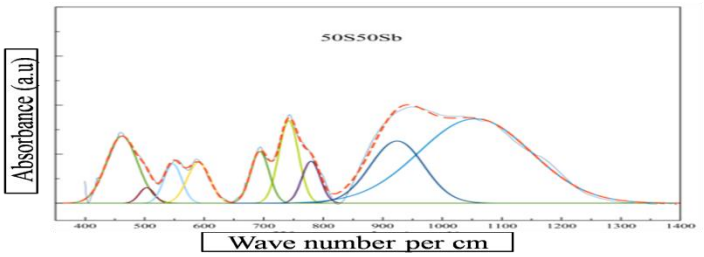

Figure 3.2(i): Deconvoluted spectra of 50S50Sb base

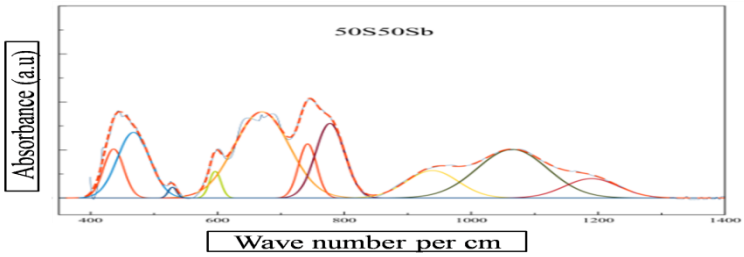

Figure 3.2(j): Deconvoluted spectra of 50S50Sb heat treated sample

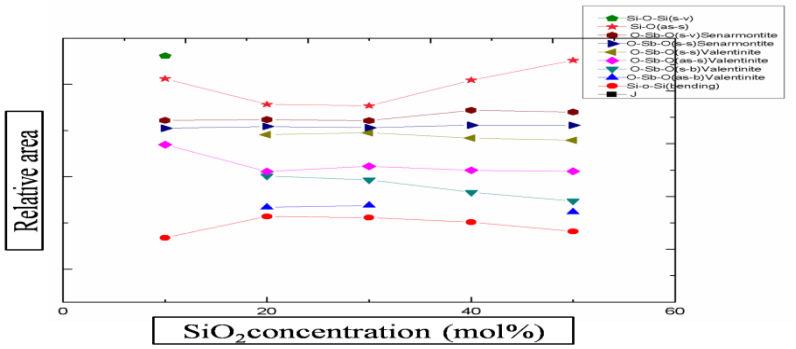

Figure 3.3(a): Relative area of the chemical bond as a function of SiO_2

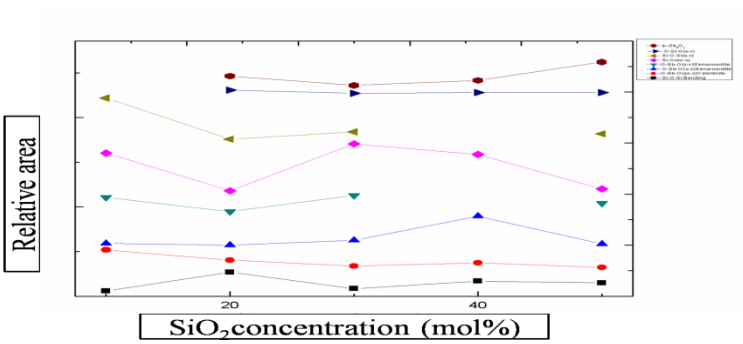

Figure 3.3(b): Relative area of the chemical bond as a function of SiO_2 of heat treated samples

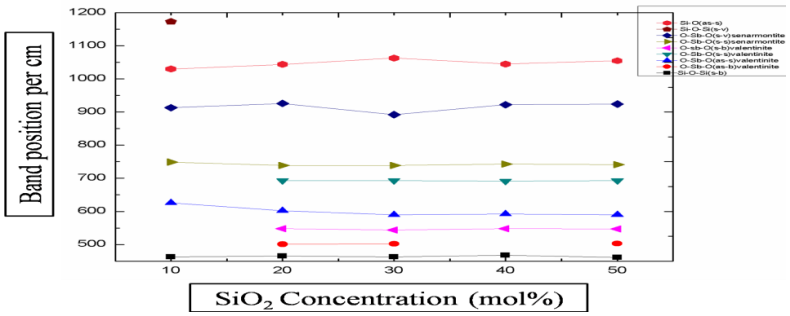

Figure 3.4(a): Variation of band position with SiO_2 concentration of base samples

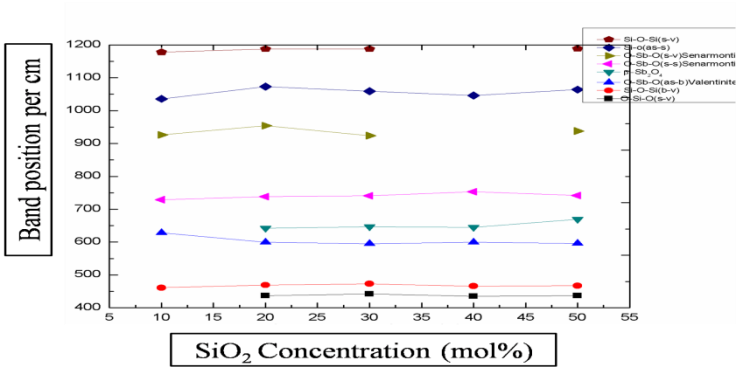

Figure 3.4(b): Variation of band position with SiO_2 concentration of heat treated samples

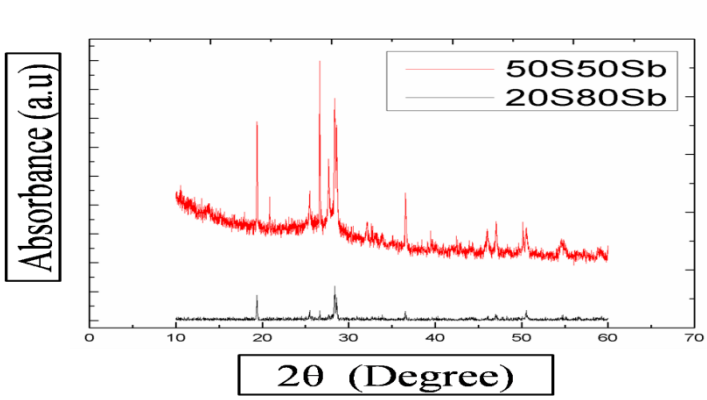

Figure 3.5(a): XRD patterns of two base samples

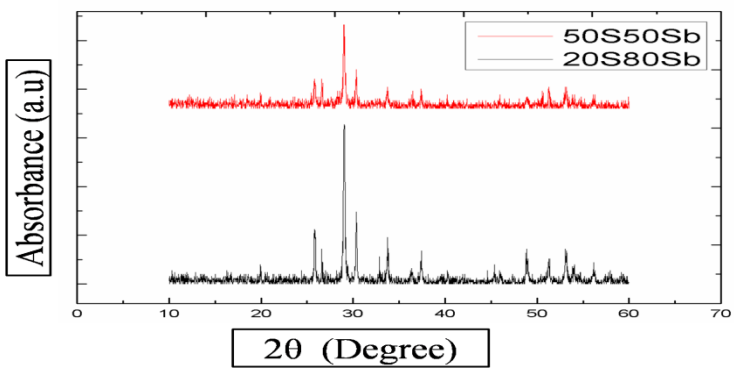

Figure 3.5(b): XRD patterns of two heat treated samples

4. Discussion

The FTIR absorbance spectra of the system $xSiO_2$ (1-x) Sb_2O_3 where x= 10%,20%,30%,40% and 50% base and heat treated glasses are shown in figure 3.1(a) and 3.1(b) respectively. From the figure we can say that the absorption intensity of the former region and later region are different. These absorption spectra exhibit some structural changes that occur in the various matrixes of the studied samples with increasing their SiO_2 content up to 50 mole%. The FTIR spectra shows, with the increasing of SiO_2 content the band positions are getting distinct excluding 30S70Sb of the base samples which shows almost same pattern as 20S80Sb. And also the absorbance intensities are decreasing with the increase of SiO_2 content. Sharpness of the band positions decreases with the increase of SiO_2.The weak band position 743cm^{-1} of 40S60Sb becomes stronger in 50S50Sb. The band position ~954cm^{-1} in 50S50Sb is getting wider with decreasing SiO_2 content. The heat treated sample, 10S90Sb shows wide and broad peaks instead of sharp peaks as same as that of the base sample. 50S50Sb of the base samples shows maximum number of band positions. The prominent band positions ~970cm^{-1} in the devitrified glasses 10S90Sb, 30S70Sb, 50S50Sb carried out at 700^{0}c are missing in the rest of the devitrified

glasses. The band positions 1384cm^{-1} is shown only at the 10S90Sb base sample and in that of the heat treated sample. The IR spectra of 30S70Sb heat treated samples are more quite different than the base samples. The band positions of the heat treated samples are shifted and broaden as well. The band positions of 20S80Sb heat treated samples are more distinct than that of the base sample and also show high absorbance intensity peaks.

The positions of the prominent absorption peaks associated with shoulder of each base and heat treated samples are summarized in Table-1. All the prominent peaks of the base and heat treated glasses are identified as strong, weak, very weak, medium and strong broad. The peaks of the heat treated glasses are shifted more with increasing SiO_2.

IR spectra seem to consist of relatively broad absorption bands and it is very difficult to identify the exact position of the absorption band. For this reason, deconvolution of these bands is considered as a useful tool to obtain the exact position of the absorption band. The band positions and widths obtained from the deconvolution are thus considered to be true representation of the spectra. Here the bands observed in the 400-1400 cm^{-1} region is deconvoluted to several Gaussians depending on the basis of spectral shape using computer program to estimate the band position and relative amounts of various bonding mechanisms. The deconvoluted spectra for samples $xSiO_2(1\text{-}x)Sb_2O_3$, $0.1 \leq x \leq 0.5$ are shown in figure 3.2. The assignments of the chemical bonds are carried out by comparing its position with the related glasses and crystalline phases. Some of these bonds are attributed to vibrations of silicate; O-H Groups, β-Sb_2O_4 and the rest are attributed to vibrations of [SbO_3] trigonal pyramid. The deconvolution process makes it possible calculate the relative area of each component bands and band positions. Each component band is related to some type of vibration in a specific structural group.

The x-ray diffraction patterns of base and heat treated samples 20S80Sb and 50S50Sb are shown in figure 3.5(a) and (b. Sharp diffraction peaks indicate highly crystalline nature of Sb_2O_3 samples [28]. The X-ray diffraction analysis shows that, depending on SiO_2 contents, this substance can be either amorphous or partially crystalline [29]. In the X-ray diffraction spectra, peak for SiO_2 is not clear which confirm the two phases of Sb_2O_3 and SiO_2 are retained in these specimens. The X-ray diffraction analysis shows that the dominant phase of Sb_2O_3 is valentinite.

5. Conclusion

In probing the structural units and changes that take place in the network with the composition of a binary or ternary glass infrared spectroscopy leads itself as an effective tool because it provides valuable information about atomic configuration and nature of chemical bonding in the glasses. The investigation of IR spectra of glasses enables to the assignment of characteristics frequencies of molecular groups in the and hence correlation of IR absorption bands with different units of various structures. The sensitivity of IR on the group frequencies give wealth information to glass ceramists. The study has clearly showed that the absorption frequencies and intensities are found to be strongly and systematically dependent on glass compositions.

Deconvolution of a band can provide the exact band position and the relative amounts of such bands, which can play an important role in structural determination. Thus IR technique can be regarded as a potential tool for present and future glass ceramists. The glasses containing Sb are highly conductive, which makes them more suitable for applications in electronics, semiconductive devices, ultra-high-speed optical switching devices, etc. Some work on this system has been done recently in which Sb_2O_3 plays the unique role of network former. In present work, we have investigated only the structural properties of Sb_2O_3-SiO_2 glass system. In future, we will try to investigate the electrical and optical properties of Sb_2O_3-SiO_2 system. As an initial the temperature coefficient of resistance (TCR) and Hall Effect measurements of one of the samples made us hopeful. Later, we have profound intension to perform all the necessary experiments which is required to investigate the semiconducting nature of our samples.

References

[1]. Dayanand C, Bhikshamiah G, Jaya, Tyagaraju V, Salagram M, Krisshana Murthy ASR, J. Mat. Sci. 31 (1996) 1945

[2]. T. Som & B. Karmokar, "Antimony Oxide Glasses and Their Nanocomposites for Optical, Photonic and Nanophotonic Applications" (CSIR, India).
[3]. H. Rawson, "Inorganic Glass Forming Systems" (Academic Press, London, 1967) p. 8. 1. H.
[4]. Carlisle, Rodney (2004). Scientific American Inventions and Discoveries, p.365. John Wright & Songs, Inc., New Jersey. ISBN 0-471-24410-4.
[5]. R. Adair et. al. J. op. Soc. Am. B, 4, 875-81 (1987).
[6]. D. W. Hall, M. A. Newhouse, N. F. Borrelli, W. H. Dom baugh and D. L. Weidman, Appl. Phys. Lett, 54,1293-95 (1995).
[7]. N. Mochida and K. Takahashi, Yogyo-Kyokaa-Shi, B4, 413-20 (1976). Systems"
[8]. Terashima et al Journal of the Ceramic Society of Japan 104 [11] 1008-1014 (1996).
[9]. C. A. Cody, L. Dicarlo, and R . K. Darlington, In. Chem., Vol. 18, No. 6, 1979
[10]. T. Som, B. Karmakar J. of Non-Cryst. Sol. 356 (2010) 987–999.
[11]. Y. Zhang et. al. J. Am. Ceram. Soc., 92 [8] 1881–1883 (2009)
[12]. M. Srinivasa Reddy, G. Murali Krishna, N. Veeraiah Journal of Physics and Chemistry of Solids 67 (2006) 789–795
[13]. Mee et al J. of Sol. St. Chem. 183 (2010) 1925–1934
[14]. Dorosz et al. Spec. Acta Part A: Mole. and Bio. Spec. 134 (2015) 608–613.
[15]. R. J. bell, N. F. Bird & P. Dean J. Phy. C.1, 299 (1968).
[16]. E. A. Hayri & M. Greenbalt, J. Non-cryst. Aolids 111,169 (1989).
[17]. F. A. Khalifa, Z. A. El-Hadi, A.A.Fl. Keshan & F.A. Mustafa, India, Pure & App. Phy. 34, 207(1195).
[18]. I. R. Beattie, K. M. S. Livingston, and D. J. Renolds, J. Chem. Soc. A 449, 51 (1970).
[19]. A. Bishay and C. Maghrabi, Phys. Chem. Glasses, 10, 1-12 (1969).
[20]. N. Allahmoradi, S. Baghshahi and M. Rajabi J. of Cer. Pro. Res. Vol. 18, No. 9, pp. 691~695 (2017).
[21]. L. Koudelka, J. Subcık, P. Mosner, L. Montagne, L. Delevoye, J. Non-Cryst. Solids 353 (2007) 1828.
[22]. S. Mandal et. al. J. of Mat. Research, Vol.15, No.1, Jan 2000.
[23]. A. A. Higazy & B. Bridge, J. Mat. Sci.20, 2345
[24]. R. M. Almedia & D. Machengie, J. Non-Cryst. Sol. 40, 535 (1980).
[25]. C. Dayanan et al. J. Mat. Sci. 31, 1945-1967 (1996).
[26]. E. G. Kalbus, Phd thesis, Winsconsin University (1957).
[27]. Z. Deng, D. Chen, F. Tang, J. Ren, A.J. Muscat, Nano Res. 2 (2009) 151.
[28]. B.S. Naidu, M. Pandey, V. Sudarsan, R.K. Vatsa, R. Tewari Chemical Physics Letters 474 (2009) 180–184.
[29]. L A. Zemnukhova, A. E. Panasenko J. of Sol. St. Chem. 201 (2013) 9–12